

# Paramagnetic–Diamagnetic Phase Transition Accompanied by Coordination Bond Formation–Dissociation in the Dithiolate Complex $\text{Na}[\text{Ni}(\text{pdt})_2] \cdot 2\text{H}_2\text{O}$

Shinya Takaishi,\* Nozomi Ishihara, Kazuya Kubo, Keiichi Katoh, Brian K. Breedlove, Hitoshi Miyasaka, and Masahiro Yamashita

Department of Chemistry, Graduate School of Science, Tohoku University, 6-3 Aza-Aoba, Aramaki, Aoba-ku, Sendai 980-8578, Japan

**S** Supporting Information

**ABSTRACT:** Bis(2,3-pyrazinedithiolate)nickel complex  $\text{Na}[\text{Ni}(\text{pdt})_2] \cdot 2\text{H}_2\text{O}$  formed one-dimensional stacks of the  $\text{Ni}(\text{pdt})_2$  units and showed strong antiferromagnetic interactions along the stacking direction. A first-order phase transition between the paramagnetic and diamagnetic states, which was driven by dimerization of the  $\text{Ni}(\text{pdt})_2$  units, accompanied by coordination bond formation, was observed.

Electronic properties of bis(*o*-dithiolate) metal complexes, such as superconductivity,<sup>1</sup> spin liquid phenomena,<sup>2</sup> single-component molecular metal behavior,<sup>3</sup> etc., have been extensively studied in relation to conducting and magnetic materials because of their redox activity and  $\pi$ -extended molecular orbitals. Some bis(*o*-dithiolate) metal complexes with a one-dimensional electronic structure undergo a phase transition caused by electronic instability or bistability via a strong electron–lattice interaction, such as a charge-transfer (CT) phase transition,<sup>4</sup> Peierls transition,<sup>5</sup> etc. In the present Communication, we report that the bis(*o*-dithiolate)nickel complex  $\text{Na}[\text{Ni}(\text{pdt})_2] \cdot 2\text{H}_2\text{O}$  (pdt = 2,3-pyrazinedithiolate) undergoes a phase transition between the paramagnetic and diamagnetic states, which is driven by dimerization of the  $\text{Ni}(\text{pdt})_2$  units, accompanied by coordination bond formation–dissociation.

$\text{Na}[\text{Ni}(\text{pdt})_2] \cdot 2\text{H}_2\text{O}$  was synthesized by the electrochemical oxidation of  $\text{Na}_2[\text{Ni}(\text{pdt})_2]$  in 5:1 (v/v)  $\text{H}_2\text{O}/\text{MeOH}$  with a constant current of 5  $\mu\text{A}$ . After 1 week, black needle-shaped crystals formed on the anode. Elem anal. Calcd for  $\text{C}_8\text{H}_8\text{N}_4\text{Na}_1\text{Ni}_1\text{O}_2\text{S}_4$ : C, 23.89; H, 2.01; N, 13.93. Found: C, 23.895; H, 1.962; N, 13.994. The magnetic susceptibility of the polycrystalline sample was measured in a 1 T field using a Quantum Design MPMS susceptometer. Single-crystal structures were determined on a Rigaku CCD diffractometer with a VariMax microfocuss X-ray source of graphite-monochromated Mo K $\alpha$  radiation ( $\lambda = 0.7107 \text{ \AA}$ ). The electrical resistivity was measured by using a two-probe method with a constant voltage of 1.0 V on a Keithley 6211 system sourcemeter.

Figure 1 shows the crystal structure of  $\text{Na}[\text{Ni}(\text{pdt})_2] \cdot 2\text{H}_2\text{O}$  at 230 K. The  $\text{Ni}(\text{pdt})_2$  units had square-planar geometries. In the *bc* plane, the  $\text{Ni}(\text{pdt})_2$  units are arranged in a herringbone motif. Each  $\text{Ni}(\text{pdt})_2$  unit is connected to each other via weak N–Na coordination bonds (N–Na distance = 2.586  $\text{\AA}$ ).  $\text{Ni}(\text{pdt})_2$  units

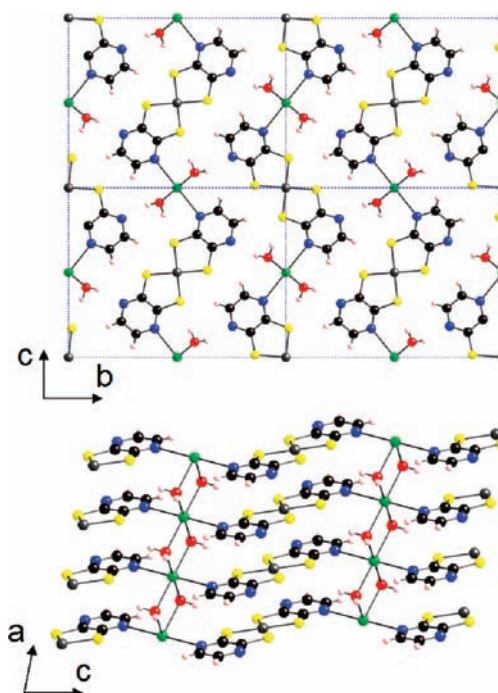


**Figure 1.** Crystal structure of  $\text{Na}[\text{Ni}(\text{pdt})_2] \cdot 2\text{H}_2\text{O}$  at 230 K: (a) top view; (b) side view. Color code: gray, Ni; yellow, S; green, Na; red, O; blue, N; black, C; pink, H.

are one-dimensionally stacked through an infinite number of  $\cdots \text{Na}-(\mu\text{-O}_{\text{aq}})_2-\text{Na} \cdots$  coordination bonds along the *a* axis with a distance of 3.54  $\text{\AA}$ , indicating that there are  $\pi$ – $\pi$  interactions between the neighboring  $\text{Ni}(\text{pdt})_2$  units. The structure is almost the same as that previously reported for  $\text{Na}[\text{Cu}(\text{pdt})_2] \cdot 2\text{H}_2\text{O}$ .<sup>6</sup> However, the nickel complex is spin  $1/2$ , whereas the copper complex is spinless.

Figure 2 shows molecular orbitals of  $[\text{Ni}(\text{pdt})_2]^-$  calculated using density functional theory (DFT) at the UB3LYP level with the 6-31G\* basis set. The X-ray data were used for the calculations, and point charges of 0.5+ were added at the positions of the Na ions. On the basis of the DFT calculations, the lowest unoccupied molecular orbital (LUMO) is comprised of an antibonding Ni  $d_{x^2-y^2}$  orbital and an S  $p_\sigma$  orbital. The singly

**Received:** April 8, 2011

**Published:** June 10, 2011

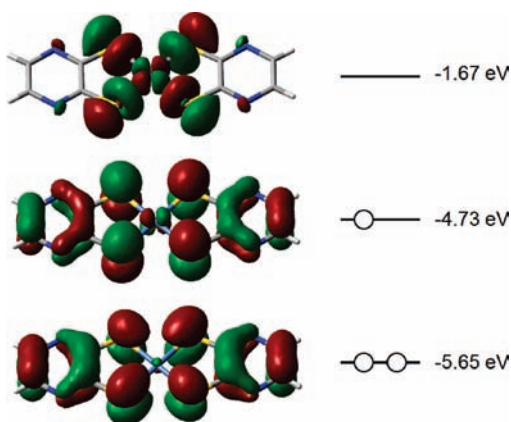


Figure 2. Frontier molecular orbitals of  $\text{Ni}(\text{pdt})_2^-$ .

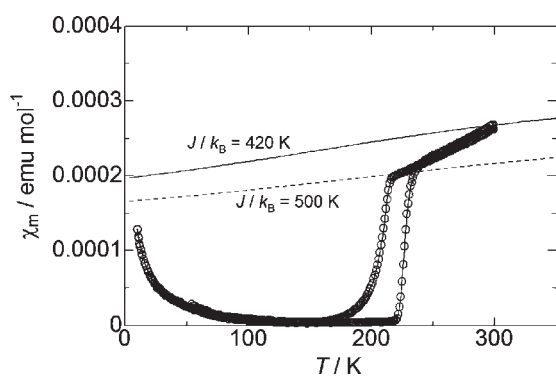


Figure 3. Magnetic susceptibility of  $\text{Na}[\text{Ni}(\text{pdt})_2] \cdot 2\text{H}_2\text{O}$ . Solid and broken lines show a Bonner–Fisher curve with  $J/k_B = 420$  and  $500$  K, respectively. An isotropic  $g$  value ( $=2.108$ ) was determined by an electron spin resonance spectrum with a methanol solution of  $\text{Na}[\text{Ni}(\text{pdt})_2] \cdot 2\text{H}_2\text{O}$ .

occupied molecular orbital (SOMO) is comprised of  $p_\pi$  orbitals on the pdt ligands with a nonnegligible contribution from the metal ion. The highest occupied molecular orbital (HOMO) is mainly comprised of  $p_\pi$  orbitals on the pdt ligands. From the crystal structure, the distance between the nearest  $\text{Ni}(\text{pdt})_2$  planes was  $3.54 \text{ \AA}$ , which means that the SOMOs of each unit  $\text{Ni}(\text{pdt})_2$  overlap, causing antiferromagnetic interactions. We also made conventional band calculations with a combination of the extended Hückel method and the tight binding model. The overlap integral ( $S$ ) between the neighboring  $\text{Ni}(\text{pdt})_2$  molecules along the stacking direction ( $=-1.05 \times 10^{-2}$ ) is much larger than that along the other direction ( $<1.5 \times 10^{-3}$ ), indicating that the present compound is nearly in a one-dimensional system.

Figure 3 shows a plot of the magnetic susceptibility of  $\text{Na}[\text{Ni}(\text{pdt})_2] \cdot 2\text{H}_2\text{O}$ . The magnetic susceptibility above  $215 \text{ K}$  gradually decreased upon cooling, indicating that strong antiferromagnetic interactions were present. The susceptibility could not be reproduced by fitting with a spin  $1/2$  one-dimensional antiferromagnetic model (Bonner–Fisher model)<sup>7</sup> with a unique  $J$  value. This is probably because the value of  $J$  itself changes with temperature between  $J/k_B = 420$  and  $500 \text{ K}$ . The magnetic susceptibility showed hysteresis at critical temperatures ( $T_c$ ) of  $216$  and  $221 \text{ K}$  upon cooling and heating, respectively. This

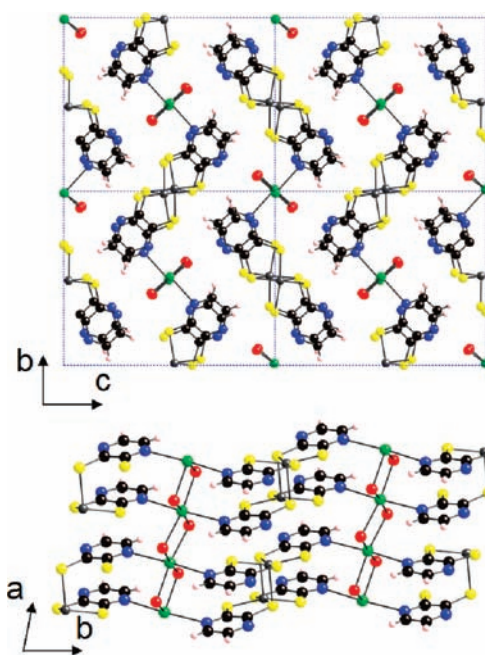


Figure 4. Crystal structure of  $\text{Na}[\text{Ni}(\text{pdt})_2] \cdot 2\text{H}_2\text{O}$  at  $210 \text{ K}$ . Color code: gray, Ni; yellow, S; green, Na; red, O; blue, N; black, C; pink, H.

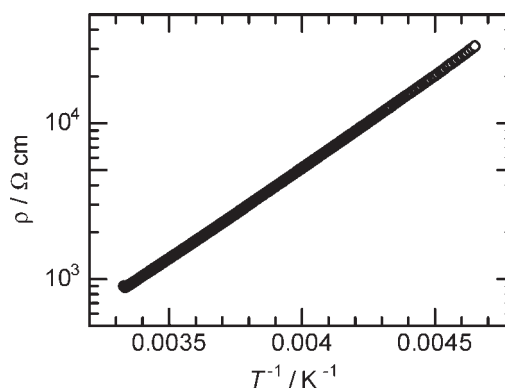


Figure 5. Electrical resistivity of  $\text{Na}[\text{Ni}(\text{pdt})_2] \cdot 2\text{H}_2\text{O}$ .

indicates that some first-order phase transitions occur between the paramagnetic and diamagnetic states.

In order to clarify the origin of the phase transition, we performed X-ray crystal structure analysis below  $T_c$  ( $210 \text{ K}$ ). The temperature was decreased from  $230$  to  $210 \text{ K}$  at a rate of  $\leq 0.5 \text{ K/min}$  because the single crystal collapsed when we decreased the temperature quickly. Figure 4 shows the crystal structure of  $\text{Na}[\text{Ni}(\text{pdt})_2] \cdot 2\text{H}_2\text{O}$  at  $210 \text{ K}$ . There was a marked difference in the molecular geometry as well as its periodicity. At  $230 \text{ K}$ , the  $\text{Ni}(\text{pdt})_2$  molecules have a mostly planar structure and were arranged uniformly, forming one-dimensional columns. At  $210 \text{ K}$ , on the other hand, the molecules were distorted from the square-planar geometry and had dimerized, forming a Ni–S coordination bond (Ni–S distance =  $2.413 \text{ \AA}$ ). The abrupt decrease in the magnetic susceptibility is explained by dimerization of the  $\text{Ni}(\text{pdt})_2$  units, which gives rise to a spin singlet ground state. The contribution of  $1/T$  at low temperature (the spin concentration is  $0.37\%$ ) is probably due to the isolated unpaired electrons arising from a phase mismatch upon dimerization.

The origin of this phase transition is qualitatively explained as follows. The tendency for dimerization in the bis(*o*-dithiolate) metal complexes highly depends on the metal ion. To the best of our knowledge, monoanionic nickel complexes have a moderate tendency to dimerize (lower than manganese, iron, and cobalt complexes and higher than copper complexes).<sup>8</sup> In the present compound, in addition, the molecules are originally arranged in a slipped stack motif to enable dimerization. Those conditions enable transformation between the monomer and dimer reversibly.

Figure 5 shows the electrical resistivity of Na[Ni(pdt)<sub>2</sub>]·2H<sub>2</sub>O. This compound showed semiconducting behavior with an activation energy of 0.23 eV above  $T_c$ . This energy gap is probably due to on-site Coulomb repulsion between the Ni-(pdt)<sub>2</sub> units. Below  $T_c$ , the electrical conductivity could not be measured because the resistivity was too high ( $>10^9 \Omega \text{ cm}$ ).

## ■ ASSOCIATED CONTENT

**S Supporting Information.** X-ray crystallographic data in CIF format and an electron spin resonance spectrum of Na[Ni-(pdt)<sub>2</sub>]·2H<sub>2</sub>O. This material is available free of charge via the Internet at <http://pubs.acs.org>.

## ■ AUTHOR INFORMATION

### Corresponding Author

\*E-mail: [takaishi@mail.tains.tohoku.ac.jp](mailto:takaishi@mail.tains.tohoku.ac.jp).

## ■ ACKNOWLEDGMENT

The authors acknowledge Dr. Shintaro Ishida and Fumiya Hirakawa for electron spin resonance measurements. This work was partly supported by a Grant-in-Aid for Creative Scientific Research from the Ministry of Education, Culture, Sports, Science and Technology.

## ■ REFERENCES

- (1) (a) Brossard, L.; Ribault, M.; Valade, L.; Cassoux, P. *J. Phys. (Paris)* **1989**, *50*, 1521–1534. (b) Brossard, L.; Ribault, M.; Valade, L.; Cassoux, P. *Physica B+C* **1986**, *143*, 378–380. (c) Schirber, J. E.; Overmyer, D. L.; Williams, J. W.; Wang, H. H.; Valade, L.; Cassoux, P. *Phys. Lett. A* **1987**, *120*, 87–88. (d) Tajima, H.; Inokuchi, M.; Kobayashi, A.; Ohta, T.; Kato, R.; Kobayashi, H.; Kuroda, H. *Chem. Lett.* **1993**, *22*, 1235–1238.
- (2) (a) Itou, T.; Oyamada, A.; Maegawa, S.; Kato, R. *Nat. Phys.* **2010**, *6*, 673–676. (b) Itou, T.; Oyamada, A.; Maegawa, S.; Tamura, M.; Kato, R. *Phys. Rev. B* **2008**, *77*, 104413.
- (3) (a) Tanaka, H.; Okano, Y.; Kobayashi, H.; Suzuki, W.; Kobayashi, A. *Science* **2001**, *291*, 285–287. (b) Kobayashi, A.; Sasa, M.; Suzuki, W.; Fujiwara, E.; Tanaka, H.; Tokumoto, M.; Okano, Y.; Fujiwara, H.; Kobayashi, H. *J. Am. Chem. Soc.* **2004**, *126*, 426–427.
- (4) (a) Torrance, L. B.; Vazquez, J. E.; Mayerle, J. J.; Lee, V. Y. *Phys. Rev. Lett.* **1981**, *46*, 253–257. (b) Umezono, Y.; Fujita, W.; Awaga, K. *J. Am. Chem. Soc.* **2006**, *128*, 1084–1085.
- (5) (a) Zeller, H. R. *J. Phys. Chem. Solids* **1974**, *35*, 77–80. (b) Jacobs, I. S.; Bray, J. W.; Hart, H. R., Jr.; Interrante, L. V.; Kasper, J. S.; Watkins, G. D.; Prober, D. E.; Bonner, J. C. *Phys. Rev. B* **1976**, *14*, 3036–3051.
- (6) Ribas, X.; Dias, J. C.; Morgado, J.; Wurst, K.; Molins, E.; Ruiz, E.; Almeida, M.; Veciana, J.; Rovira, C. *Chem.—Eur. J.* **2004**, *10*, 1691–1704.
- (7) (a) Bonner, J. C.; Fisher, M. E. *Phys. Rev. A* **1964**, *135*, 640–658. (b) Estes, W. E.; Gavel, D. P.; Hatfield, W. E.; Hodgson, D. J. *Inorg. Chem.* **1978**, *17*, 1415–1421.
- (8) Karlin, K. D.; Stiefel, E. I. *Progress in Inorganic Chemistry*; John Wiley & Sons, Inc.: New York, 2004; Vol. 52.